ACS OMEGA

Article

Cite This: ACS Omega 2019, 4, 18002−18010

http://pubs.acs.org/journal/acsodf

Passivation of Layered Gallium Telluride by Double Encapsulation with Graphene

Elisha Mercado,*,† Yan Zhou,*,† Yong Xie,‡ Qinghua Zhao,§ Hui Cai,∥ Bin Chen,∥ Wanqi Jie,§ Sefaattin Tongay,∥ Tao Wang,§ and Martin Kuball*,†

†Center for Device Thermography and Reliability (CDTR), H. H. Wills Physics Laboratory, University of Bristol, Tyndall Avenue, Bristol BS8 1TL, U.K.

‡School of Advanced Materials and Nanotechnology, Key Laboratory of Wide Band-Gap Semiconductor Materials and Devices, Xidian University, Xi'an 710071, P. R. China

§State Key Laboratory of Solidification Processing, Northwestern Polytechnical University, Xi'an 710072, P. R. China

∥School for Engineering of Matter, Transport and Energy, Arizona State University, Tempe, Arizona 85287, United States

Supporting Information

ABSTRACT: Layered semiconductor gallium telluride (GaTe) undergoes a rapid structural transition to a degraded phase in ambient conditions, limiting its utility in devices such as optical switches. In this work, we demonstrate that the degradation process in GaTe flakes can be slowed down dramatically via encapsulation with graphene. Through examining Raman signatures of degradation, we show that the choice of substrate significantly impacts the degradation rate and that the process is accelerated by the transfer of GaTe to hydrophilic substrates such as SiO_2/Si. We find that double encapsulation with both top and bottom graphene layers can extend the lifetime of the material for several weeks. The photoresponse of flakes encapsulated in this way is only reduced by 17.6 ± 0.4% after 2 weeks, whereas unencapsulated flakes display no response after this time. Our results demonstrate the potential for alternative, van der Waals material-based passivation strategies in unstable layered materials and highlight the need for careful selection of substrates for 2D electronic devices.

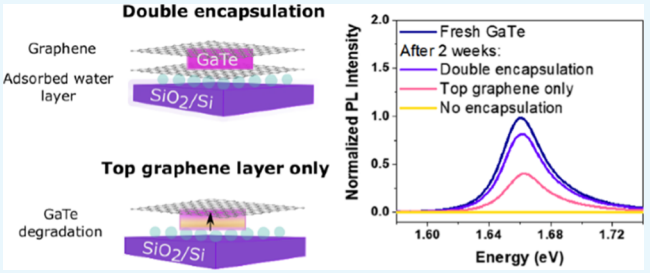

INTRODUCTION

III−VI monochalcogenides are a relatively unexplored part of the layered semiconductor family with the intralayer structure X−M−M−X, where M is a group III element (Ga, In) and X is a chalcogen (S, Se, Te). Materials in this group are mostly hexagonal, with the exception of Te-based compounds which crystallize in a lower symmetry monoclinic form.[1] GaSe has gained popularity in recent years because of its strong optical absorption and potential for applications in nonlinear optics.[2−4] GaTe has recently begun to generate significant interest as a possible alternative for optoelectronic devices because it displays much stronger absorptivity than GaSe.[5] Unlike other layered materials such as the transition-metal dichalcogenides,[6] the moderate bandgap of GaTe (1.65 eV)[7] remains direct from the monolayer to bulk form, allowing for greater flexibility in selecting the thickness of the photoactive layer. GaTe photodetectors with high photoresponsivities (10^4 A/W), fast photoresponse times (6 ms) and detectivities (10^{12} jones) exceeding those of even commercial InGaAs detectors[8] have been demonstrated.[9,10] More recently, scalable, low-residue solution-processed GaTe devices have been fabricated with photoresponsivities as high as 2×10^6 A/W.[11] Additionally, unintentional p-type doping[12] in GaTe presents opportunities for p−n heterojunction devices with n-type 2D materials such as MoS_2.[13,14] GaTe also demonstrates very high levels of in-plane anisotropy, reflected in its electronic and optical properties.[15−17] However, progress in GaTe-based devices has been hindered by poor environmental stability.[18,19]

2D materials are especially prone to environmental instability because of their high surface area to volume ratio. The most frequently studied unstable 2D material to date is few-layered black phosphorus (BP), desirable for its high hole mobility,[20] moderate bandgap,[21] and strong optical and electrical anisotropy.[22] Despite this, degradation of BP-based devices remains a significant issue. The reaction proceeds mainly via photooxidation, with a rate that is dependent on flake thickness, oxygen concentration, and illumination power.[23] Rate of degradation in BP has also previously been shown to be impacted by substrate choice.[24]

Tellurium-based layered compounds such as GaTe degrade via a more complex oxidation reaction. O_2 intercalates between the layers and forms bonds with highly reactive Te atoms,

Received: June 13, 2019
Accepted: September 5, 2019
Published: October 25, 2019

DOI: 10.1021/acsomega.9b01752
ACS Omega 2019, 4, 18002−18010

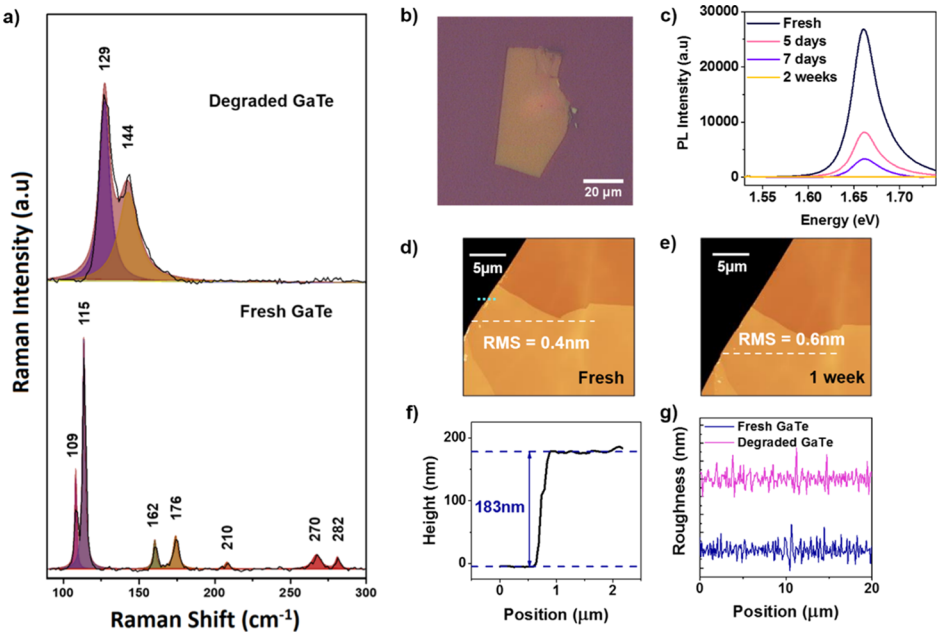

Figure 1. Degradation signatures in GaTe. (a) Raman spectrum of freshly exfoliated GaTe (bottom) and fully degraded GaTe after 7 days (top). (b) Optical image of a GaTe flake transferred to SiO_2/Si substrate. (c) PL spectra of freshly exfoliated GaTe and after 5, 7, and 14 days of ambient exposure. AFM topography of (d) fresh and (e) fully degraded sample after 7 days. Blue dotted line in (d) shows location of the flake height profile shown in (f) and white dashed lines show the position of roughness profiles in (g).

leading to a structural transition to an oxide phase, confirmed via Raman spectroscopy, photoluminescence (PL) spectroscopy, and energy-dispersive X-ray spectroscopy.[19,25] This reaction is catalyzed by water and does not occur in dry air.[26] The transition to the oxide phase leads to the loss of optical anisotropy and a reduction in bandgap from 1.65 eV to approximately 0.8 eV. This process can be partially reversed by annealing to drive out adsorbed O_2 between GaTe layers.[26] A number of strategies have been proposed to slow the oxidation process, including surface functionalization with diazonium molecules[19] and encapsulation with passivation layers such as Al_2O_3.[25]

Despite improvements to the environmental stability of these materials using conventional oxides such as Al_2O_3,[25,27−29] there are several problems associated with the deposition of these layers on 2D materials. The lack of dangling bonds at 2D interfaces may necessitate the inclusion of a seeding layer or pretreatment[29−31] to facilitate nucleation, while the deposition process itself has been found to be a cause of increased degradation at the surface in very thin samples.[32] Additionally, because of the extreme sensitivity of 2D materials to external perturbations, these passivation layers can alter the intrinsic electronic properties of the target materials significantly[33] and prevent access to novel materials engineering capabilities via surface modification.[34,35] Al_2O_3 passivation may also limit applications for 2D materials in optical electronics and wearable devices by adversely impacting their mechanical flexibility and optical transparency.[36] As a result, encapsulation with other van der Waals materials has emerged as a possible alternative to conventional passivation layers. Interfaces between 2D materials are atomically sharp and can be self-cleaning.[37] Van der Waals passivation in this way also has the advantage that the capping layer could be selected to enhance the desirable qualities of the material while simultaneously acting as a protective layer. This has previously been realized for BP and graphene or hexagonal boron nitride (h-BN)-based devices.[38] More recently, few-layer GaSe has been stabilized under ambient conditions via capping with h-BN.[39] To the best of our knowledge, this type of passivation is yet to be demonstrated with GaTe.

Here, we demonstrate a method for monitoring the degradation level of GaTe flakes using Raman spectroscopy and present a strategy to slow this reaction via van der Waals passivation with graphene. Additionally, we show that deposition of GaTe flakes onto conventional dielectric layers (SiO_2) accelerates oxidation, likely due to the hydrophilicity of the substrate. We show that as a result, the addition of a hydrophobic buffer layer such as graphene at the bottom GaTe surface is required for effective passivation. We find that sandwiching GaTe with graphene extends the lifetime of the material greatly, with only minimal oxidation occurring after 2 weeks. Because previous theoretical studies have indicated that graphene/GaTe heterostructures have the potential to combine high photoabsorption with ballistic electronic transport in optoelectronic devices,[40,41] this passivation strategy presents an opportunity to employ graphene layers as both a protective layer and active component of the heterostructure which has important implications for future device fabrication.

RESULTS AND DISCUSSION

GaTe flakes were exfoliated from a bulk crystal onto SiO_2/Si substrates and characterized using micro-Raman spectroscopy, PL, and atomic force microscopy (AFM). Figure 1a shows the Raman spectrum of freshly cleaved and degraded GaTe. The freshly cleaved sample shows prominent peaks at 109, 115, 162, 176, 210, 270, and 283 cm^{-1} in good agreement with previous reports.[25,26,42] Aged flakes exhibit only two peaks at 129 and 144 cm^{-1}. The origin of these modes is still the subject of some controversy. Some previous first-principles calculations have suggested that these modes can be attributed to first[42] or second-order[15] Raman-active phonon modes, whereas other groups have claimed that they appear only as the

DOI: 10.1021/acsomega.9b01752
ACS Omega 2019, 4, 18002−18010

products of the GaTe oxidation process.[19,25,26] In the latter case, the similarities to both TeO_2 and aged Raman spectra of other Te-containing compounds have been noted,[19] supporting the idea that the 129 and 144 cm^{-1} peaks result from the oxidation of Te atoms at the sample surface.[26] In our work, we attribute these peaks to degradation products because they are either totally absent or extremely weak in freshly exfoliated samples and only emerge following prolonged exposure to air.

The evolution of pristine to aged GaTe is evident from the loss of the PL signal over time (Figure 1c). Freshly exfoliated samples exhibit a strong photoresponse centered at 1.66 eV, which is consistent with the reported bandgap of GaTe.[7] The peak intensity decreases with longer ambient exposure times, leading to a complete loss of the signal after around 2 weeks. This is reflective of a transition from a direct gap material to the indirect gap oxide phase.[26] AFM topography scans comparing a freshly exfoliated and one week old GaTe are shown in Figure 1d,e. A small increase in root mean square (rms) roughness from 0.4 to 0.6 nm is observed as a result of the transition to the oxide phase. The optical appearance of the flakes is unchanged. Our findings are consistent with previous reports and suggest that unlike other unstable layered materials such as BP,[38] surface roughness is not a good indicator of the level of sample degradation in GaTe.

Because we found the changes in the Raman spectrum of GaTe with ambient exposure to be the most significant sign of degradation, we used Raman spectroscopy to probe the degree of sample degradation over time. Figure 2a shows the evolution

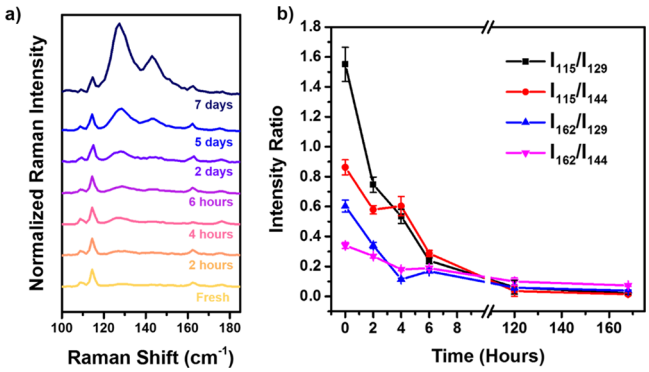

Figure 2. Evolution of GaTe Raman signatures of a 183 nm GaTe flake over time. (a) Measured Raman spectra at various ambient exposure times. Spectra have been normalized to 115 cm^{-1} mode peak intensity for clarity. (b) Comparison of I_{115}/I_{129}, I_{162}/I_{129}, I_{115}/I_{144}, and I_{162}/I_{144} intensity ratios as a function of ambient exposure time.

of Raman spectra over time for a 183 nm thick GaTe flake in air. After only a few hours, peaks attributed to the oxide phase began to appear, of which the 129 cm^{-1} mode was the most pronounced. As the flake continued to oxidize, a marked increase in the intensity of the 129 and 144 cm^{-1} oxide peaks was observed in addition to a reduction in intensity of the GaTe-attributed modes. After 7 days, almost all GaTe peaks had disappeared and only the oxide peaks remained, indicating a complete transition to the degraded GaTe phase. We studied the integrated intensity ratios of the Raman peaks attributed to GaTe and the oxide phase over time to develop a metric for the degree of sample degradation. Figure 2b shows a comparison of I_{115}/I_{129}, I_{162}/I_{129}, I_{115}/I_{144}, and I_{162}/I_{144} intensity ratios as a function of ambient exposure time. Smaller ratios indicate a greater degree of degradation. A rapid decrease in all ratios was observed during the first few hours of ambient exposure, followed by a slower progression to complete oxidization, indicated by an intensity ratio of zero, after several days. This is suggestive of saturation of the GaTe layers with chemisorbed O_2 with increasing ambient exposure. Although each ratio displayed the same trend, we identified I_{115}/I_{129} as the best metric for sample comparisons. The 115 cm^{-1} peak is the strongest and last GaTe mode to disappear with degradation, while the 129 cm^{-1} oxide peak emerges earlier in the oxidation process than the 144 cm^{-1} mode. The I_{115}/I_{129} ratio is therefore a clearer indicator of the levels of degradation over the full range of exposure times.

To improve the environmental stability of GaTe flakes via van der Waals layer passivation, we tested two types of the GaTe/graphene heterostructure to determine whether graphene is an effective encapsulation layer for GaTe. Single encapsulated samples were capped by a single graphene flake (7 nm) transferred on top of ~175 nm GaTe so that it was completely covered. Double encapsulated structures were fabricated in the same way but with the addition of an extra graphene layer (7 nm) underneath the GaTe flake. All samples were exfoliated from bulk crystals and transferred onto SiO_2/Si substrates (see Experimental Section). Figure 3a shows the three assembly steps used to fabricate graphene/GaTe/graphene sandwich structures. Optical images, AFM topography, and height profiles for each layer are shown in Figure 3b–d, e–g, and h–j for steps 1–3, respectively. For single encapsulated flake fabrication, the same process was followed starting from step 2, with the deposition of GaTe directly onto the SiO_2 surface. Sample degradation over time was monitored using Raman spectroscopy, and we confirmed the evolution of optoelectronic properties with ambient exposure using PL.

Optical images of the single and double encapsulated samples are shown in Figure 4a,b, respectively. Thicknesses of all layers were confirmed in each case using AFM. Raman spectra for graphene layers (Figure 4c) in each case agree well with literature reports for multilayer graphene[44] and the absence of the defect-activated D peak suggests high material quality.[45] Raman spectra as a function of ambient exposure time for single and double encapsulated samples are shown in Figure 4d,e. Both samples showed reduced degradation compared with bare GaTe which was fully oxidized after 7 days. By contrast, both graphene encapsulated samples still exhibit GaTe Raman modes at 115 and 162 cm^{-1}, suggesting that neither were fully degraded even after 2 weeks. The single encapsulated sample showed a much higher level of oxidation than the double encapsulated, with a mean I_{115}/I_{129} ratio of 0.22 ± 0.06 after 2 weeks. However, the double encapsulated flake seemed relatively unaffected even after this time, as only very small oxidation peaks were observed. After 2 weeks, the mean I_{115}/I_{129} ratio was measured as 1.71 ± 0.17, nearly 8 times larger than the single encapsulated flake. Compared with unencapsulated flakes, this ratio was slightly larger than the average measured for even freshly transferred samples (Figure 2b). We suggest that this was a result of a small amount of oxidation on contact with SiO_2/Si for the unencapsulated material.

The superior passivation properties of double versus single graphene encapsulation of GaTe can also be seen from the PL spectra in Figure 4d. The photoresponse of the single encapsulated flake was reduced by around 60.4 ± 0.6%, while the double encapsulated sample experienced only a 17.6

DOI: 10.1021/acsomega.9b01752
ACS Omega 2019, 4, 18002−18010

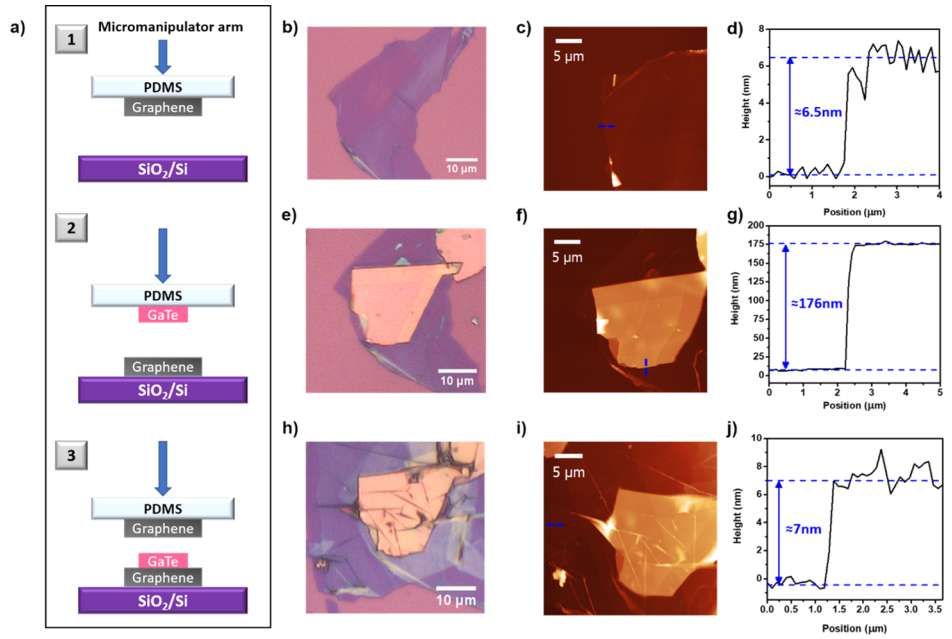

Figure 3. Assembly of graphene/GaTe/graphene sandwich structures on SiO_2/Si. (a) Outline of the deposition process. Flakes are exfoliated onto a viscoelastic poly-dimethyl siloxane (PDMS) stamp before being loaded into a micromanipulator. The stamping process is carried out in the order shown in the schematic using the procedure first reported by Castellanos-Gomez et al.[43] (b,e,h) Optical images of typical structures after step 1, 2, and 3, respectively. AFM topography of structures following step 1 (c), 2 (f), and 3 (i). Blue dashed lines show locations of height scans of the most recently added layer as shown in (d,g,j).

± 0.4% intensity loss after 2 weeks. This represents a significant improvement over unencapsulated GaTe flakes which exhibit no photoresponse after this time.

The origin of this effect is not immediately clear. Because the top interfaces of both the double and single encapsulated flakes are identical, we suggest that it must be due to the difference between the bottom GaTe interfaces with either graphene or SiO_2, respectively. To investigate this further, we transferred ∼175 nm GaTe flakes onto various substrates to compare the resulting rates of degradation. Bare SiO_2/Si and Al-coated SiO_2 were chosen as primary substrates, and chemical vapor deposition (CVD) graphene monolayers were transferred onto both to determine the impact of the addition of bottom graphene layers on the degradation rate. Optical images of flakes on each of the substrates tested can be found in the Supporting Information (S1). SiO_2/Si was chosen because of its popularity as a substrate in 2D device fabrication, while the smoother Al-coated substrate was used as a means of investigating potential roughness effects. The rms roughness of SiO_2/Si and Al-coated SiO_2/Si substrates were measured as 0.21 and 0.13 nm, respectively (Supporting Information, S2). It was thought that the increased substrate roughness could lead to poor contact between the GaTe flake and the substrate, allowing for increased diffusion of O_2 and moisture from air along this interface. In this case, a faster degradation rate on substrates with higher surface roughness would be expected. Figure 5a shows Raman spectra of monolayer graphene on SiO_2/Si and Al-coated SiO_2/Si substrates. The presence of the D peak at ≈1375 cm^{-1} in both samples indicates some degree of structural disorder in the graphene layers. However, the small D to G (≈1580 cm^{-1}) peak intensity ratios indicate that the defect level is still relatively low in both samples[46] (I_D/I_G = 0.15 for SiO_2/Si and I_D/I_G = 0.14 for Al). The monolayer character of graphene transferred to both substrates was confirmed by the single Lorentzian lineshape of the 2D Raman peak (≈2700 cm^{-1}) and small G to 2D peak intensity ratios (I_G/I_{2D} = 0.21 for SiO_2/Si and I_G/I_{2D} = 0.29 for Al).[44]

A comparison of the I_{115}/I_{129} peak intensity ratio for all substrates is shown in Figure 5b. We observed that the degradation rate for SiO_2/Si and Al substrates was virtually identical, and GaTe flakes transferred onto these surfaces were again fully degraded after 1 week. This suggests that substrate roughness is not a significant factor in GaTe sample degradation. Placing a graphene buffer layer between the substrate and GaTe led to a slower transition to the oxide phase on both substrates. Again, the rates for graphene/SiO_2/Si and graphene/Al are not significantly different. It was noted that the intensity ratios of fresh flakes transferred to the bare substrates were significantly lower than the fresh flakes on graphene, again suggesting that some degree of oxidation had occurred upon contact with SiO_2/Si or Al substrates. We observed that the 115 cm^{-1} peak was still visible for the graphene/SiO_2/Si sample even after 3 weeks, suggesting that the lifetime of a GaTe flake and potential GaTe-based devices can be extended simply by a careful choice of the substrate.

We also tested the use of mechanically exfoliated multilayer graphene flakes as a substrate for GaTe (see Supporting Information, S3). The exfoliated graphene substrate flakes were found to provide superior protection to the GaTe compared with the CVD monolayers shown here, possibly due to a lower level of structural defects or the presence of poly(methyl methacrylate) (PMMA) residues on the monolayer surfaces left over from the transfer process. To test the influence of polymer residues on the degradation rate of GaTe, flakes were transferred to monolayer graphene surfaces with high and low levels of PMMA residue (Supporting Information, S4). We observed that higher residue levels led to increased degradation in GaTe, possibly due to further decomposition of residues into oxygen-containing products.[47,48]

DOI: 10.1021/acsomega.9b01752
ACS Omega 2019, 4, 18002−18010

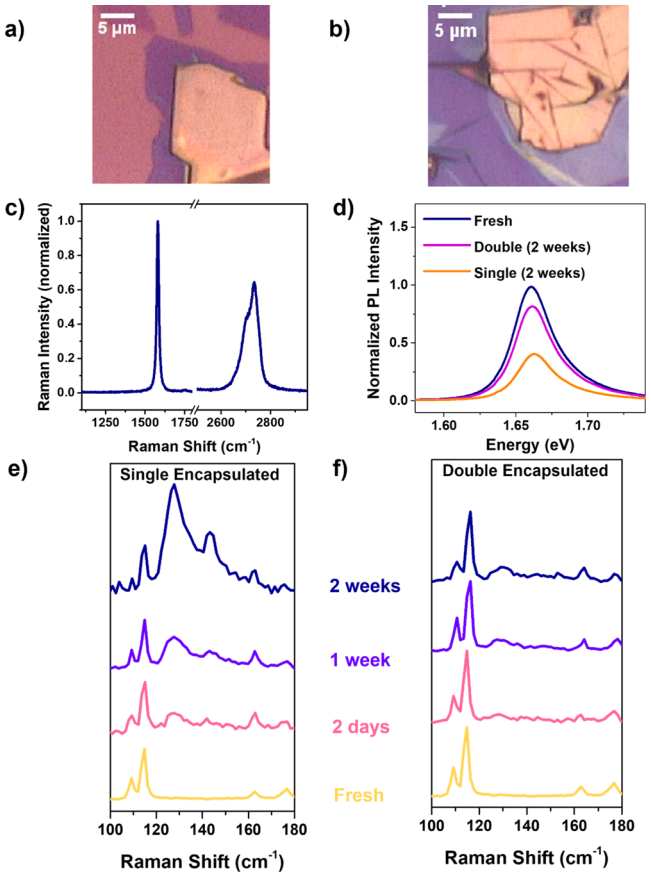

Figure 4. Comparison of degradation rates for double and single encapsulated GaTe. Optical images of single encapsulated (a), and double encapsulated (b) GaTe flakes. (c) Typical Raman spectrum of multilayer graphene samples used for encapsulation. (d) PL measurements of fresh and 2 week-old single and double encapsulated flakes with graphene. Double and single encapsulation spectra have been normalized to the peak intensity of the fresh samples for the purposes of comparison. Raman spectra evolution over time for GaTe (e) single encapsulated and (f) double encapsulated with graphene.

Degradation in GaTe is thought to proceed by intercalation of molecular oxygen between layers in the presence of moist air.[26] Because the top interface is identical for all samples (GaTe/air), there must be some feature of the SiO_2/Si and Al substrates that encourages this process compared with graphene substrates. It has already been established above that substrate roughness is likely not a factor; therefore there must be some other origin for this effect. One possibility is that the variation in degradation rates is due to the differences in the wettability of the underlying substrates. This effect has already been observed for BP flakes,[24] although the degradation mechanism for BP is not the same as that for GaTe. Figure 5c–f shows contact angle measurements for our substrates both covered and uncovered with graphene. SiO_2/Si and Al substrates are both hydrophilic ($\theta_{SiO_2} = 61.51° \pm 0.19°$ and $\theta_{Al} = 68.37 \pm 0.35°$ respectively) in agreement with previous literature reports.[49,50] It is well known that hydrophilic surfaces lead to the formation of water adlayers under ambient conditions.[51] We suggest that adsorbed water on the SiO_2/Si and Al substrates is trapped at the interface after deposition of GaTe, resulting in progressive degradation due to the presence of dissolved O_2. As we observed from direct transfer of GaTe to these substrates, this can result in some level of immediate oxidation on contact for fresh flakes. Diffusion of water adlayers along 2D-material/SiO_2 interfaces has been previously demonstrated with graphene.[52] The mechanism is such that even if only a small amount of water is trapped initially, the volume may increase after flake deposition due to capillary forces attracting water molecules from surrounding areas. Over time, it is therefore possible for additional adsorbed moisture and O_2 to be drawn along the substrate surface under the GaTe flake, degrading the sample even further.

We suggest that the addition of a graphene buffer layer between the GaTe and the substrate causes the water layer to instead be trapped at the substrate–graphene interface, avoiding contact with the GaTe flake. Our contact angle measurements show that deposition of a graphene monolayer on the bare substrate surfaces renders them both hydrophobic (Figure 5d,f). Although recent experiments have shown that it is possible for water to be adsorbed on hydrophobic surfaces under ambient conditions,[53] particularly at defect sites, the area of the substrate covered by adsorbed water is significantly smaller than that for a hydrophilic substrate. It therefore seems likely that a smaller volume of adsorbed water may be trapped and drawn along a hydrophobic substrate/GaTe boundary than a hydrophilic one, leading to a reduction in the degradation rate on hydrophobic surfaces. This suggests that in order to fully realize the potential of GaTe as an alternative for electronic devices, hydrophobic substrates to the common choice of SiO_2/Si are required.

To further test the role of substrate wettability on the degradation rate of GaTe, we transferred fresh ∼175 nm flakes onto SiO_2/Si cleaned using standard solvent cleaning methods and SiO_2/Si treated with a plasma cleaning process. Details of both treatments can be found in the Experimental Section. Plasma cleaning increases the substrate wettability significantly due to more effective removal of organic contaminants.[54] We found the substrate/water contact angle was reduced to less than 30° following plasma treatment. Figure 6a,b shows the evolution of Raman spectra of ∼175 nm GaTe flakes on solvent-cleaned and plasma-cleaned SiO_2/Si, respectively. Fresh GaTe transferred to the plasma-cleaned substrate was clearly degraded on contact to a greater extent than the flake transferred to the solvent-rinsed sample, as can be seen from the much stronger 129 cm^{-1} peak. This is consistent with the presence of an increased volume of adsorbed water on the substrate surface prior to transfer. Additionally, the plasma-cleaned sample was almost fully degraded after just two days, suggesting that oxidation occurs much more rapidly on the more hydrophilic surface. This was confirmed via tracking the ratio of I_{115}/I_{129} peaks over time as shown in Figure 6c.

The potential for applications of GaTe/graphene heterostructures has been previously highlighted elsewhere,[41] particularly for photodetector and radiation detector devices.[40] Despite this, no such devices have yet been realized. This work demonstrates that the fabrication of air-stable GaTe/graphene-based devices may be possible without the need for direct exposure of GaTe to complex and potentially damaging processes for deposition of conventional encapsulation layers.[29−32] Photodetectors employing sandwich-type structures with graphene similar to those presented here have already been demonstrated for MoS_2.[55] A similar device employing GaTe as the active layer may offer improved photoresponsivity and faster response times,[9−11] while the graphene layers have the potential to both improve charge

DOI: 10.1021/acsomega.9b01752
ACS Omega 2019, 4, 18002−18010

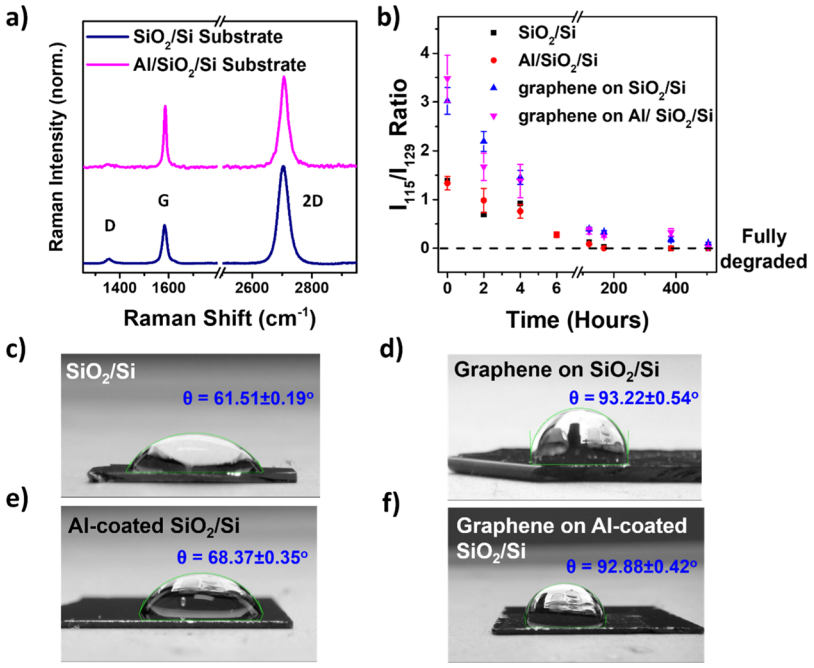

Figure 5. Comparison of degradation rates on different substrates. (a) Raman spectra of graphene monolayers on SiO_2/Si and Al/SiO_2/Si substrates showing D, G, and 2D peaks at ≈1375, 1580^{-}, and 2700 cm^{-1}, respectively. (b) I_{115}/I_{129} intensity ratios as a function of time for SiO_2/Si, Al-coated SiO_2/Si, graphene on SiO_2/Si, and graphene on Al-coated SiO_2/Si. (c–f) Contact angle measurements for (c) SiO_2/Si (θ = 61.51 ± 0.19°), (d) graphene on SiO_2/Si (θ = 93.22 ± 0.54°), (e) Al-coated SiO_2/Si (θ = 68.37 ± 0.35°), and (f) graphene on Al-coated SiO_2/Si (θ = 92.88 ± 0.42°).

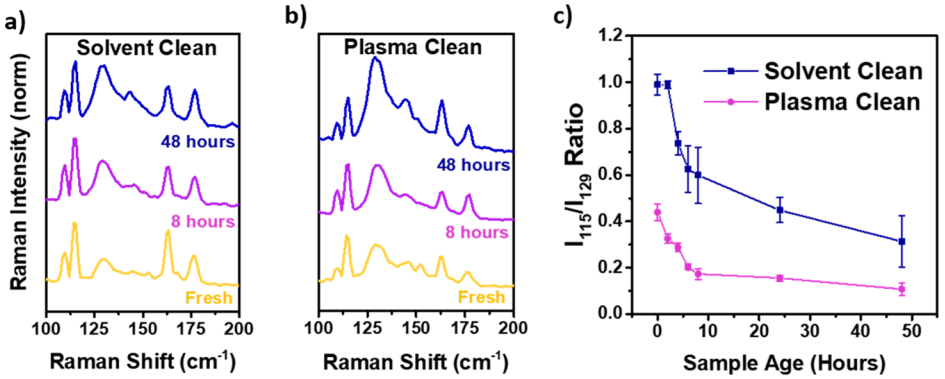

Figure 6. Comparison of degradation rates of GaTe on solvent-cleaned and plasma-cleaned SiO_2/Si. (a,b) Measured Raman measurements of GaTe on (a) solvent-cleaned and (b) plasma-cleaned substrates over time. (c) I_{115}/I_{129} intensity ratio as a function of time.

transport and protect GaTe from environmental degradation. h-BN has also previously been employed as a 2D-material-based passivation layer[38,39] and is known to be hydrophobic.[56] The use of h-BN as an alternative dielectric, coupled with graphene as a charge transport layer presents ample opportunities for stable GaTe-based device fabrication, particularly in the field of flexible devices where the limiting factor is often the failure of conventional dielectric or encapsulation layers such as Al_2O_3.[57,58]

CONCLUSIONS

We investigated the potential for van der Waals passivation of GaTe using graphene and quantified the level of degradation using Raman spectroscopy. Encapsulation with graphene slows oxidation significantly, leading to only a minimal reduction in flake photoresponse even after 2 weeks. However, we found that capping GaTe on SiO_2 with only a top layer of graphene is only partially effective and an additional buffer layer at the bottom interface is required to further slow oxidation. We suggest that this effect is due to the hydrophilicity of the substrate, observing that the degradation rate can be tuned via substrate wettability. These results have important implications for improving the environmental stability of GaTe-based devices and suggest a need for hydrophobic alternatives to conventional SiO_2 dielectric layers.

EXPERIMENTAL SECTION

Sample Preparation and Characterization. Single-crystal GaTe bulk ingot was grown via modified Bridgman method using high purity gallium (99.9999%, Alfa Aesar) and tellurium (99.9999%, Alfa Aesar) powders mixed in a 1:1 stoichiometry. GaTe flakes were mechanically exfoliated from bulk single crystals onto a PDMS stamp (Sylgard 184 Elastomer kit, Sigma-Aldrich). The approximate thickness of

DOI: 10.1021/acsomega.9b01752
ACS Omega 2019, 4, 18002−18010

the flakes was estimated by optical contrast in order to identify candidates for transfer of a suitable thickness (~175 nm). Care was also taken to select flakes of similar lateral dimensions (approximately 20 μm by 20 μm) for fair comparison between samples. Flakes were transferred onto the target substrate via a viscoelastic stamping process.[43] Moderate heating (50 °C) of the target substrate was necessary to facilitate the process. For fresh samples, Raman measurements were carried out immediately post-transfer. Graphene flakes were exfoliated and transferred using a method identical to the above from bulk HOPG purchased from Alfa Aesar. The thickness of transferred GaTe and graphene flakes were determined via AFM measurements (Bruker Dimension Edge).

To study substrate-dependent degradation, commercially available graphene monolayers precoated with PMMA (Graphenea) grown via CVD were used. This was necessary to provide a sufficiently large area of coverage for contact angle measurements. These samples were transferred to target substrates via a wet etching method. Copper foil substrates were etched using a 0.1 M ammonium persulfate (Sigma-Aldrich) solution and the graphene/PMMA stack was transferred to a bath of water for cleaning. After spreading the graphene sheet onto the target substrate, samples were left to dry in a fume cupboard overnight. The PMMA support was then removed by submerging in acetone for 12 h, followed by rinsing with isopropyl alcohol (IPA) and drying in N_2.

Raman Spectroscopy and PL Measurements. Raman and PL measurements were carried out using a Renishaw InVia Raman spectrometer using a 488 nm laser excitation. Error bars in all calculated intensity ratios represent one standard deviation from the mean of at least five different measurements. In all cases, the incident power was kept below 0.5 mW to avoid laser-induced sample degradation.

Substrate Contact Angle Measurements. SiO_2 (300 nm)/Si and Al-coated (80 nm) SiO_2/Si substrates were cleaned in a standard process by successive rinsing in acetone and IPA, followed by drying in N_2. Plasma-cleaning of SiO_2/Si was performed on an Oxford Instruments PlasmaLab 100 System for 60 s at 40 °C and a pressure of 30 mTorr using 20 sccm O_2 and 100 W RF power. The chamber was then purged with 40 sccm Ar gas for 2 min.

For contact angle measurements, a droplet of H_2O was deposited onto the substrate to be tested and the solid−liquid interface was imaged with a digital camera. The image was processed in ImageJ using the dropanalysis plugin[59] (LBADSA technique) to extract the contact angle. The contact angles extracted represent the mean of three trials for each substrate.

■ ASSOCIATED CONTENT

Supporting Information

The Supporting Information is available free of charge on the ACS Publications website at DOI: 10.1021/acsomega.9b01752.

Optical images of GaTe flakes on various substrates, substrate roughness profiles and AFM topography scans, comparison of the GaTe degradation rate on CVD monolayers and 7 and 22 nm exfoliated graphene flakes, and impact of the PMMA residue level on the GaTe degradation rate (PDF)

■ AUTHOR INFORMATION

Corresponding Authors

*E-mail: elisha.mercado@bristol.ac.uk (E.M.).
*E-mail: yan.zhou@bristol.ac.uk (Y.Z.).
*E-mail: martin.kuball@bristol.ac.uk (M.K.).

ORCID

Elisha Mercado: 0000-0003-0399-5077
Yan Zhou: 0000-0001-6470-6991
Sefaattin Tongay: 0000-0001-8294-984X

Author Contributions

The manuscript was written through contributions of all authors. All authors have given approval to the final version of the manuscript. E.M., Y.Z., and M.K. initiated the project and designed the experiments. E.M. performed experimental measurements and analyzed the data. Y.Z. assisted with sample preparation and characterization. Y.X., Q.Z., H.C., B.C., W.J., S.T., and T.W. grew the bulk crystals. M.K. supervised the project.

Notes

The authors declare no competing financial interest.

■ ACKNOWLEDGMENTS

E.M. acknowledges funding and support from the Engineering and Physical Sciences Research Council (EPSRC) Centre for Doctoral Training in Condensed Matter Physics (CDT-CMP), grant no. EP/L015544/1.

■ REFERENCES

(1) Fong, C. Y.; Schlüter, M. *Electrons and Phonons in Layered Crystal Structures*, 1st ed.; Wieting, T. J., Schlüter, M., Eds.; Springer Netherlands: Dordrecht, 1979; pp.145−315.

(2) Hu, P.; Wen, Z.; Wang, L.; Tan, P.; Xiao, K. Synthesis of Few-Layer GaSe Nanosheets for High Performance Photodetectors. *ACS Nano* **2012**, *6*, 5988−5994.

(3) Karvonen, L.; Säynätjoki, A.; Mehravar, S.; Rodriguez, R. D.; Hartmann, S.; Zahn, D. R. T.; Honkanen, S.; Norwood, R. A.; Peyghambarian, N.; Kieu, K.; et al. Investigation of Second- and Third-Harmonic Generation in Few-Layer Gallium Selenide by Multiphoton Microscopy. *Sci. Rep.* **2015**, *5*, 10334.

(4) Jie, W.; Chen, X.; Li, D.; Xie, L.; Hui, Y. Y.; Lau, S. P.; Cui, X.; Hao, J. Layer-Dependent Nonlinear Optical Properties and Stability of Non-Centrosymmetric Modification in Few-Layer GaSe Sheets. *Angew. Chem., Int. Ed.* **2015**, *54*, 1185−1189.

(5) Camassel, J.; Merle, P.; Mathieu, H.; Gouskov, A. Near-band-edge optical properties ofGaSexTe1−xmixed crystals. *Phys. Rev. B: Condens. Matter Mater. Phys.* **1979**, *19*, 1060−1068.

(6) Wang, Q. H.; Kalantar-Zadeh, K.; Kis, A.; Coleman, J. N.; Strano, M. S. Electronics and Optoelectronics of Two-Dimensional Transition Metal Dichalcogenides. *Nat. Nanotechnol.* **2012**, *7*, 699−712.

(7) Brebner, J. L.; Fischer, G.; Mooser, E. Optical Absorption Edge of GaTe. *J. Phys. Chem. Solids* **1962**, *23*, 1417−1421.

(8) Konstantatos, G.; Howard, I.; Fischer, A.; Hoogland, S.; Clifford, J.; Klem, E.; Levina, L.; Sargent, E. H. Ultrasensitive Solution-Cast Quantum Dot Photodetectors. *Nature* **2006**, *442*, 180−183.

(9) Liu, F.; Shimotani, H.; Shang, H.; Kanagasekaran, T.; Zólyomi, V.; Drummond, N.; Fal'ko, V. I.; Tanigaki, K. High-Sensitivity Photodetectors Based on Multilayer GaTe Flakes. *ACS Nano* **2014**, *8*, 752−760.

(10) Hu, P.; Zhang, J.; Yoon, M.; Qiao, X.-F.; Zhang, X.; Feng, W.; Tan, P.; Zheng, W.; Liu, J.; Wang, X.; et al. Highly Sensitive Phototransistors Based on Two-Dimensional GaTe Nanosheets with Direct Bandgap. *Nano Res.* **2014**, *7*, 694−703.

DOI: 10.1021/acsomega.9b01752
ACS Omega 2019, 4, 18002−18010

(11) Kang, J.; Sangwan, V. K.; Lee, H.-S.; Liu, X.; Hersam, M. C. Solution-Processed Layered Gallium Telluride Thin-Film Photodetectors. *ACS Photonics* **2018**, *5*, 3996−4002.
(12) Tatsuyama, C.; Watanabe, Y.; Hamaguchi, C.; Nakai, J. Some Optical Properties of Layer-Type Semiconductor GaTe. *J. Phys. Soc. Jpn.* **1970**, *29*, 150−155.
(13) Yang, S.; Wang, C.; Ataca, C.; Li, Y.; Chen, H.; Cai, H.; Suslu, A.; Grossman, J. C.; Jiang, C.; Liu, Q.; et al. Self-Driven Photodetector and Ambipolar Transistor in Atomically Thin GaTe-MoS2 p-n vdW Heterostructure. *ACS Appl. Mater. Interfaces* **2016**, *8*, 2533−2539.
(14) Wang, F.; Wang, Z.; Xu, K.; Wang, F.; Wang, Q.; Huang, Y.; Yin, L.; He, J. Tunable GaTe-MoS $_2$ van Der Waals P−n Junctions with Novel Optoelectronic Performance. *Nano Lett.* **2015**, *15*, 7558−7566.
(15) Huang, S.; Tatsumi, Y.; Ling, X.; Guo, H.; Wang, Z.; Watson, G.; Puretzky, A. A.; Geohegan, D. B.; Kong, J.; Li, J.; et al. In-Plane Optical Anisotropy of Layered Gallium Telluride. *ACS Nano* **2016**, *10*, 8964−8972.
(16) Shenoy, U. S.; Gupta, U.; Narang, D. S.; Late, D. J.; Waghmare, U. V.; Rao, C. N. R. Electronic Structure and Properties of Layered Gallium Telluride. *Chem. Phys. Lett.* **2016**, *651*, 148−154.
(17) Susoma, J.; Karvonen, L.; Säynätjoki, A.; Mehravar, S.; Norwood, R. A.; Peyghambarian, N.; Kieu, K.; Lipsanen, H.; Riikonen, J. Second and Third Harmonic Generation in Few-Layer Gallium Telluride Characterized by Multiphoton Microscopy. *Appl. Phys. Lett.* **2016**, *108*, 073103.
(18) Williams, R. H.; McEvoy, A. J. Surface Properties of the Gallium Monochalcogenides. *Phys. Status Solidi* **1972**, *12*, 277−286.
(19) Yang, S.; Cai, H.; Chen, B.; Ko, C.; Özçelik, V. O.; Ogletree, D. F.; White, C. E.; Shen, Y.; Tongay, S. Environmental Stability of 2D Anisotropic Tellurium Containing Nanomaterials: Anisotropic to Isotropic Transition. *Nanoscale* **2017**, *9*, 12288−12294.
(20) Li, L.; Yu, Y.; Ye, G. J.; Ge, Q.; Ou, X.; Wu, H.; Feng, D.; Chen, X. H.; Zhang, Y. Black Phosphorus Field-Effect Transistors. *Nat. Nanotechnol.* **2014**, *9*, 372−377.
(21) Tran, V.; Soklaski, R.; Liang, Y.; Yang, L. Layer-Controlled Band Gap and Anisotropic Excitons in Few-Layer Black Phosphorus. *Phys. Rev. B: Condens. Matter Mater. Phys.* **2014**, *89*, 235319.
(22) Xia, F.; Wang, H.; Jia, Y. Rediscovering Black Phosphorus as an Anisotropic Layered Material for Optoelectronics and Electronics. *Nat. Commun.* **2014**, *5*, 4458.
(23) Favron, A.; Gaufrès, E.; Fossard, F.; Phaneuf-L'Heureux, A.-L.; Tang, N. Y.-W.; Lévesque, P. L.; Loiseau, A.; Leonelli, R.; Francoeur, S.; Martel, R. Photooxidation and Quantum Confinement Effects in Exfoliated Black Phosphorus. *Nat. Mater.* **2015**, *14*, 826−832.
(24) Wood, J. D.; Wells, S. A.; Jariwala, D.; Chen, K.-S.; Cho, E.; Sangwan, V. K.; Liu, X.; Lauhon, L. J.; Marks, T. J.; Hersam, M. C. Effective Passivation of Exfoliated Black Phosphorus Transistors against Ambient Degradation. *Nano Lett.* **2014**, *14*, 6964−6970.
(25) Susoma, J.; Lahtinen, J.; Kim, M.; Riikonen, J.; Lipsanen, H. Crystal Quality of Two-Dimensional Gallium Telluride and Gallium Selenide Using Raman Fingerprint. *AIP Adv.* **2017**, *7*, 015014.
(26) Fonseca, J. J.; Tongay, S.; Topsakal, M.; Chew, A. R.; Lin, A. J.; Ko, C.; Luce, A. V.; Salleo, A.; Wu, J.; Dubon, O. D. Bandgap Restructuring of the Layered Semiconductor Gallium Telluride in Air. *Adv. Mater.* **2016**, *28*, 6465−6470.
(27) Luo, X.; Rahbarihagh, Y.; Hwang, J. C. M.; Liu, H.; Du, Y.; Ye, P. D. Temporal and Thermal Stability of Al $_2$ O $_3$ -Passivated Phosphorene MOSFETs. *IEEE Electron Device Lett.* **2014**, *35*, 1314−1316.
(28) Illarionov, Y. Y.; Waltl, M.; Rzepa, G.; Knobloch, T.; Kim, J.-S.; Akinwande, D.; Grasser, T. Highly-Stable Black Phosphorus Field-Effect Transistors with Low Density of Oxide Traps. *npj 2D Mater. Appl.* **2017**, *1*, 23.
(29) Wells, S. A.; Henning, A.; Gish, J. T.; Sangwan, V. K.; Lauhon, L. J.; Hersam, M. C. Suppressing Ambient Degradation of Exfoliated InSe Nanosheet Devices via Seeded Atomic Layer Deposition Encapsulation. *Nano Lett.* **2018**, *18*, 7876−7882.
(30) Azcatl, A.; McDonnell, S.; Peng, X.; Dong, H.; Qin, X.; Addou, R.; Mordi, G. I.; Lu, N.; Kim, J.; et al. MoS $_2$ Functionalization for Ultra-Thin Atomic Layer Deposited Dielectrics. *Appl. Phys. Lett.* **2014**, *104*, 111601.
(31) McDonnell, S.; Pirkle, A.; Kim, J.; Colombo, L.; Wallace, R. M. Trimethyl-Aluminum and Ozone Interactions with Graphite in Atomic Layer Deposition of Al $_2$ O $_3$. *J. Appl. Phys.* **2012**, *112*, 104110.
(32) Zhu, H.; McDonnell, S.; Qin, X.; Azcatl, A.; Cheng, L.; Addou, R.; Kim, J.; Ye, P. D.; Wallace, R. M. Al $_2$ O $_3$ on Black Phosphorus by Atomic Layer Deposition: An *in Situ* Interface Study. *ACS Appl. Mater. Interfaces* **2015**, *7*, 13038−13043.
(33) Liu, H.; Neal, A. T.; Si, M.; Du, Y.; Ye, P. D. The Effect of Dielectric Capping on Few-Layer Phosphorene Transistors: Tuning the Schottky Barrier Heights. *IEEE Electron Device Lett.* **2014**, *35*, 795−797.
(34) Hu, T.; Hong, J. First-Principles Study of Metal Adatom Adsorption on Black Phosphorene. *J. Phys. Chem. C* **2015**, *119*, 8199−8207.
(35) Niu, T.; Zhang, J.; Chen, W. Surface Engineering of Two-Dimensional Materials. *ChemNanoMat* **2019**, *5*, 6−23.
(36) Kuriakose, S.; Ahmed, T.; Balendhran, S.; Bansal, V.; Sriram, S.; Bhaskaran, M.; Walia, S. Black Phosphorus: Ambient Degradation and Strategies for Protection. *2D Mater* **2018**, *5*, 032001.
(37) Novoselov, K. S.; Mishchenko, A.; Carvalho, A.; Castro Neto, A. H. 2D Materials and van Der Waals Heterostructures. *Science* **2016**, *353*, aac9439.
(38) Doganov, R. A.; O'Farrell, E. C. T.; Koenig, S. P.; Yeo, Y.; Ziletti, A.; Carvalho, A.; Campbell, D. K.; Coker, D. F.; Watanabe, K.; Taniguchi, T.; et al. Transport Properties of Pristine Few-Layer Black Phosphorus by van Der Waals Passivation in an Inert Atmosphere. *Nat. Commun.* **2015**, *6*, 6647.
(39) Zhao, Q.; Frisenda, R.; Gant, P.; Perez de Lara, D.; Munuera, C.; Garcia-Hernandez, M.; Niu, Y.; Wang, T.; Jie, W.; Castellanos-Gomez, A. Toward Air Stability of Thin GaSe Devices: Avoiding Environmental and Laser-Induced Degradation by Encapsulation. *Adv. Funct. Mater.* **2018**, *28*, 1805304.
(40) Olmos-Asar, J. A.; Leão, C. R.; Fazzio, A. Novel III-Te-graphene van der Waals heterojunctions for optoelectronic devices. *RSC Adv.* **2017**, *7*, 32383−32390.
(41) Li, H.; Zhou, Z.; Zhang, K.; Wang, H. Schottky Barrier Modulation of a GaTe/graphene Heterostructure by Interlayer Distance and Perpendicular Electric Field. *Nanotechnology* **2019**, *30*, 405207.
(42) Wang, T.; Zhao, Q.; Miao, Y.; Ma, F.; Xie, Y.; Jie, W. Lattice Vibration of Layered GaTe Single Crystals. *Crystals* **2018**, *8*, 74.
(43) Castellanos-Gomez, A.; Buscema, M.; Molenaar, R.; Singh, V.; Janssen, L.; van der Zant, H. S. J.; Steele, G. A. Deterministic Transfer of Two-Dimensional Materials by All-Dry Viscoelastic Stamping. *2D Mater* **2014**, *1*, 011002.
(44) Ferrari, A. C.; Basko, D. M. Raman Spectroscopy as a Versatile Tool for Studying the Properties of Graphene. *Nat. Nanotechnol.* **2013**, *8*, 235−246.
(45) Thomsen, C.; Reich, S. Double Resonant Raman Scattering in Graphite. *Phys. Rev. Lett.* **2000**, *85*, 5214.
(46) Cançado, L. G.; Jorio, A.; Ferreira, E. H. M.; Stavale, F.; Achete, C. A.; Capaz, R. B.; Moutinho, M. V. O.; Lombardo, A.; Kulmala, T. S.; Ferrari, A. C. Quantifying Defects in Graphene via Raman Spectroscopy at Different Excitation Energies. *Nano Lett.* **2011**, *11*, 3190−3196.
(47) Parts, L.; Hardy, E. E.; Rodenburg, M. L. Laser Radiation-Induced, Residue-Free, Localized Decomposition Of Some Plastics. *Ind. Eng. Chem. Prod. Res. Dev.* **1970**, *9*, 21−26.
(48) Jia, Y.; Gong, X.; Peng, P.; Wang, Z.; Tian, Z.; Ren, L.; Fu, Y.; Zhang, H. Toward High Carrier Mobility and Low Contact Resistance: Laser Cleaning of PMMA Residues on Graphene Surfaces. *Nano-Micro Lett.* **2016**, *8*, 336−346.
(49) Williams, R.; Goodman, A. M. Wetting of Thin Layers of SiO $_2$ by Water. *Appl. Phys. Lett.* **1974**, *25*, 531−532.

DOI: 10.1021/acsomega.9b01752
ACS Omega 2019, 4, 18002−18010

(50) Bernardin, J. D.; Mudawar, I.; Walsh, C. B.; Franses, E. I. Contact Angle Temperature Dependence for Water Droplets on Practical Aluminum Surfaces. *Int. J. Heat Mass Transfer* **1997**, *40*, 1017−1033.
(51) Verdaguer, A.; Sacha, G. M.; Bluhm, H.; Salmeron, M. Molecular Structure of Water at Interfaces: Wetting at the Nanometer Scale. *Chem. Rev.* **2006**, *106*, 1478−1510.
(52) Temmen, M.; Ochedowski, O.; Schleberger, M.; Reichling, M.; Bollmann, T. R. J. Hydration Layers Trapped between Graphene and a Hydrophilic Substrate. *New J. Phys.* **2014**, *16*, 053039.
(53) Cao, P.; Xu, K.; Varghese, J. O.; Heath, J. R. The Microscopic Structure of Adsorbed Water on Hydrophobic Surfaces under Ambient Conditions. *Nano Lett.* **2011**, *11*, 5581−5586.
(54) Gupta, V.; Madaan, N.; Jensen, D. S.; Kunzler, S. C.; Linford, M. R. Hydrogen Plasma Treatment of Silicon Dioxide for Improved Silane Deposition. *Langmuir* **2013**, *29*, 3604−3609.
(55) Yu, W. J.; Liu, Y.; Zhou, H.; Yin, A.; Li, Z.; Huang, Y.; Duan, X. Highly Efficient Gate-Tunable Photocurrent Generation in Vertical Heterostructures of Layered Materials. *Nat. Nanotechnol.* **2013**, *8*, 952−958.
(56) Li, H.; Zeng, X. C. Wetting and Interfacial Properties of Water Nanodroplets in Contact with Graphene and Monolayer Boron-Nitride Sheets. *ACS Nano* **2012**, *6*, 2401−2409.
(57) Zhu, W.; Yogeesh, M. N.; Yang, S.; Aldave, S. H.; Kim, J.-S.; Sonde, S.; Tao, L.; Lu, N.; Akinwande, D. Flexible Black Phosphorus Ambipolar Transistors, Circuits and AM Demodulator. *Nano Lett.* **2015**, *15*, 1883−1890.
(58) Zhu, W.; Park, S.; Yogeesh, M. N.; McNicholas, K. M.; Bank, S. R.; Akinwande, D. Black Phosphorus Flexible Thin Film Transistors at Gighertz Frequencies. *Nano Lett.* **2016**, *16*, 2301−2306.
(59) Stalder, A. F.; Kulik, G.; Sage, D.; Barbieri, L.; Hoffmann, P. A Snake-Based Approach to Accurate Determination of Both Contact Points and Contact Angles. *Colloids Surf., A* **2006**, *286*, 92−103.

DOI: 10.1021/acsomega.9b01752
ACS Omega 2019, 4, 18002−18010